

## Asymmetric Hollow Nanorod Formation through a Partial Galvanic Replacement Reaction

Daeha Seo and Hyunjoon Song\*

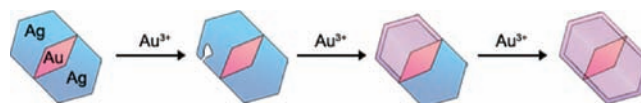
Department of Chemistry, Korea Advanced Institute of Science and Technology, Daejeon 305-701, Korea

Received September 9, 2009; E-mail: hsong@kaist.ac.kr

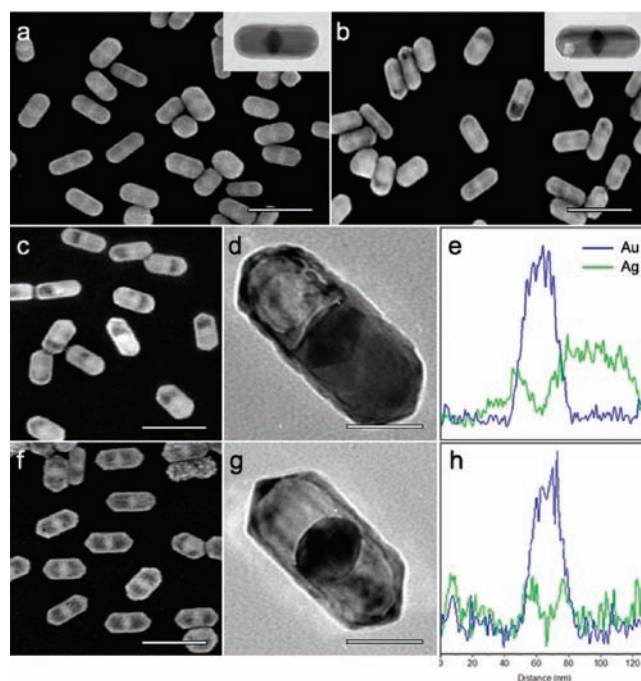
Hollow nanostructures or nanocages have been used as carriers for site-specific drug delivery.<sup>1</sup> In particular, metal nanocages are of critical interest because of their surface plasmon extinctions in the near-IR (NIR) range,<sup>2</sup> which efficiently penetrate into biological media. Metal nanocages are commonly synthesized by metal layer deposition and the subsequent removal of templates.<sup>3</sup> Xia and co-workers<sup>4</sup> developed nanoscale galvanic replacement reactions, where Ag nanostructures were displaced by other noble metals to form metal hollows. However, most of the hollow structures were restricted to highly symmetrical structures, including hollow spheres, vacant regular polyhedrons, and tubes. In the present work, asymmetric hollow formation is demonstrated for the first time in a heterometal nanorod system by a partial galvanic replacement reaction. Careful control of the reaction kinetics could yield a single hollow on one end as well as a double hollow on both ends of the silver domain in the Ag–Au–Ag nanorod structure.

Figure 1 shows the sequence of galvanic replacement in a single heterometal nanorod upon the addition of  $\text{Au}^{3+}$ . The Ag–Au–Ag nanorods were synthesized through directional growth of silver on gold decahedrons.<sup>5</sup> The resulting structure is a rod with an average aspect ratio of  $2.3 \pm 0.4$  (diameter,  $61 \pm 8$  nm; length,  $140 \pm 10$  nm) (Figure 2a). Each rod has  $C_2$  symmetry, as the silver domain is divided into two parts by the gold decahedron at the center. When a small amount of  $\text{HAuCl}_4$  solution was added into the aqueous rod dispersion, a single pit was generated on one end of the silver domain in the nanorods, as clearly observed in the transmission electron microscopy (TEM) image (Figure 2b inset). The pit position on each rod is rather arbitrary, meaning that the reaction is not specific to the crystallographic facets (Figure S1 in the Supporting Information). Increasing the gold precursor concentration yielded a vacancy continuously grown from the pit that approached the full area of one end of the rod structure. The scanning electron microscopy (SEM) image in Figure 2c shows that the left and right ends of each nanorod could be distinguished by contrast. The TEM image of a single rod (Figure 2d) indicates that a thin metal shell maintained the original nanorod framework, but one end of the nanorod was completely empty. The metal shell was single-crystalline and composed of a Au/Ag alloy (Au 27%, Ag 73%) (Figure S2). The energy-dispersive X-ray spectroscopy (EDX) line profile along the long axis confirms the asymmetrical nature of the hollow position. In Figure 2e, the intensity of the silver composition (green trace) is definitely asymmetric, in contrast to that of the gold (blue trace), which is centered on the nanorod.

Further increases in the gold precursor concentration yielded double-hollow nanorods (Figure 2f). The nanorod framework is still preserved as an elongated decahedron having flat walls and sharp tips by thin Au/Ag alloy shells with an average thickness of  $6 \pm 1$  nm. The inner vacant areas are divided into two sections by the gold particles connected to the framework. The gold particles in the center have an ellipsoidal shape as a result of residual silver (or Au/Ag alloy) layers on the particle surface (Figure 2g). The



**Figure 1.** Schematic representation of the galvanic replacement in a Ag–Au–Ag heterometal nanorod.



**Figure 2.** SEM and TEM (insets) images of (a) original heterometal nanorods and (b) hollow structures produced by the addition of 0.02 mL of the gold precursor solution. (c, f) SEM and (d, g) TEM images and (e, h) EDX line profiles along the long axes of the hollow structures produced by the addition of (c–e) 0.04 and (f–h) 0.10 mL of the gold precursor solution. The bars represent (a, b, c, f) 200 and (d, g) 50 nm.

EDX line profile along the rod long axis in Figure 2h shows that the silver and gold intensities are symmetrical with respect to the center position. When more gold precursor solution was added, the metal frameworks crumbled into small pieces (Figure S3).

The mechanism of the galvanic replacement reactions was suggested for silver nanostructures.<sup>4</sup> Our experiment is along the lines of this descriptive reaction mechanism. However, symmetry breaking and the formation of asymmetric hollows are rather striking because the galvanic replacement reaction does not have any site or surface preference. One interesting example is the controlled pore generation at the truncated corners of the silver cubes, where the {111} facets selectively react with the gold precursor to form a regular hole arrangement.<sup>6</sup> In this case, the site specificity was rooted in the preferential {100} surface covering by poly(vinyl

pyrrolidone) rather than the replacement reaction itself. In our experiment, the Ag–Au–Ag nanorods have two distinct silver sections, one on each side of the central gold decahedron, and the reaction randomly began at one of the silver sections in the nanorod structure. Therefore, the key point for asymmetry is the formation of only a single pit at the beginning of galvanic replacement. At the early stages of the reaction, gold is evenly deposited on the silver surface in an epitaxial fashion because of the low lattice mismatch (0.19%) between silver and gold. The resulting gold layers can effectively cover the silver surface to prevent replacement reactions at multiple positions. After generation of a pit on the surface, the pit acts as an active site where exposed Ag(0) is readily oxidized to Ag<sup>+</sup>. Further replacement occurs only at the pit and causes expansion of the hole up to the size of a single Ag section, yielding a single-hollow structure without damaging the other silver region. Another plausible factor is the effective electron transfer from the hole to the rod surface. The electrons generated from the oxidation of Ag(0) to Ag<sup>+</sup> at the pit are transferred to the rod surface through conductive media (silver and gold domains); the Au<sup>3+</sup> ions in solution are then reduced to Au(0) and evenly deposited on the surface. Even if another pit is concurrently generated, this electron transfer can increase the local oxidation potential of silver and reduce the activity of the replacement reaction at that position.

The gold nanocages show intense extinctions in the NIR range.<sup>2</sup> In the UV–vis–NIR spectra, the Ag–Au–Ag heterometal nanorods exhibit peaks at 410 nm (transverse mode of the Ag domain) and 500 nm (transverse mode of the Au domain) as well as a broad shoulder at 610 nm (longitudinal mode of domain coupling) (Figure S4). When a small amount of the gold precursor is added, the former peaks at 410 and 500 nm remain unchanged, but the latter peak at 610 nm suddenly shifts to 660 nm because of the gold layer deposition. The asymmetric single hollow rods (Figure 2c) show the two peaks of the Ag and Au transverse modes and a shoulder centered at 660 nm, which may be a mode from the residual Au–Ag rod structure. The rods also have a unique peak centered at 960 nm, which is in good agreement with those of gold hollow cubes and spheres over a range of 800–1000 nm. The double-hollow rods (Figure 2f) exhibit two characteristic peaks at 830 and 1250 nm, which are assignable to modes of the anisotropic hollow structure, as well as the transverse mode of the central gold particles at 540 nm. The Ag transverse mode disappears in this spectrum, reflecting the complete removal of the pure silver domains. It is noticeable that the hollow morphology precisely determines the optical properties in the NIR range, although the outer metal framework is nearly identical in the single- and double-hollow rods.

Galvanic replacement reactions with different compositions are also applicable for this heterometal nanorod system. With H<sub>2</sub>PtCl<sub>6</sub> as a platinum precursor, the present reaction conditions yielded a double-hollow structure with a rodlike platinum framework bearing gold particles inside (Figure 3a,b and Figure S5). The entire structure and dimensions are almost identical to those of the gold double-hollow rods, except for a rough Pt surface. The HRTEM image of the outer shell (Figure 3c) shows that the surface contains many defects with separate silver and platinum lattice domains, having distances between adjacent lattice fringes of 0.209 nm for Ag(200) and 0.228 nm for Pt(111). This is reasonable on the basis of the large lattice mismatch (4.00%) between silver and platinum, which can lead to irregular deposition of platinum species on the surface. In this reaction, asymmetric hollow

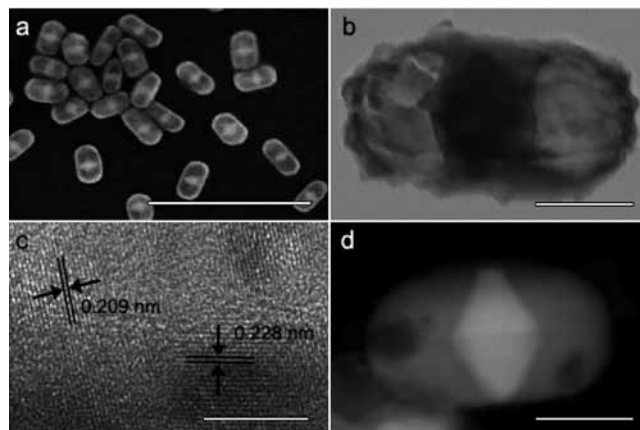


**Figure 3.** (a) SEM, (b) TEM, and (c) HRTEM images of the double hollow nanorods by the addition of 0.10 mL of the platinum precursor solution, and (d) HAADF-STEM image of a nanorod by the addition of 0.015 mL of the platinum precursor solution. The bars represent (a) 500 nm, (b,d) 50 nm, and (c) 5 nm.

nanorods did not form at all, and multiple hole formation was simultaneously observed at an early stage of the replacement reaction, as shown in high-angle annular dark-field scanning transmission electron microscopy (HAADF-STEM), SEM, and TEM images (Figure 3d and Figure S6).

In conclusion, asymmetric single-hollow and symmetric double-hollow nanorods were generated from Ag–Au–Ag heterometal nanorods by partial galvanic replacement reactions. The symmetry breaking occurs as a result of the random generation of a single pit on one end of the Ag domain. Such control of hollow formation with variable NIR extinctions will be helpful in biorelated applications such as chemical delivery, imaging, and photothermal therapy.<sup>2,7</sup>

**Acknowledgment.** This work was supported by the Pioneer Research Program under Contract 2008-05103 and by the National Research Foundation, funded by the Korean Government (MEST) (R11-2007-050-04002-0).

**Supporting Information Available:** Experimental procedures; TEM, HRTEM, HAADF-STEM, and SEM images and EDX and UV–vis–NIR spectra of the different stages of the galvanic replacement reactions. This material is available free of charge via the Internet at <http://pubs.acs.org>.

## References

- Peer, D.; Karp, J. M.; Hong, S.; Farokhzad, O. C.; Margalit, R.; Langer, R. *Nat. Nanotechnol.* **2007**, *2*, 751.
- (a) Chen, J.; Wiley, B.; Li, Z.-Y.; Campbell, D.; Saeki, F.; Cang, H.; Au, L.; Lee, J.; Li, X.; Xia, Y. *Adv. Mater.* **2005**, *17*, 2255. (b) Halas, N. J. *MRS Bull.* **2005**, *30*, 362. (c) Hirsch, L. R.; Stafford, R. J.; Bankson, J. A.; Sershen, S. R.; Rivera, B.; Price, R. E.; Hazle, J. D.; Halas, N. J.; West, J. L. *Proc. Natl. Acad. Sci. U.S.A.* **2003**, *100*, 13549.
- Lou, X. W.; Archer, L. A.; Yang, Z. *Adv. Mater.* **2008**, *20*, 3987.
- (a) Sun, Y.; Mayers, B.; Xia, Y. *Adv. Mater.* **2003**, *15*, 641. (b) Sun, Y.; Xia, Y. *J. Am. Chem. Soc.* **2004**, *126*, 3892. (c) Lu, X.; Tuan, H.-Y.; Chen, J.; Li, Z.-Y.; Korgel, B. A.; Xia, Y. *J. Am. Chem. Soc.* **2007**, *129*, 1733.
- Seo, D.; Yoo, C. I.; Jung, J.; Song, H. *J. Am. Chem. Soc.* **2008**, *130*, 2940.
- Chen, Y.; McLellan, J. M.; Siekkinen, A.; Xiong, Y.; Li, Z.-X.; Xia, Y. *J. Am. Chem. Soc.* **2006**, *128*, 14776.
- (a) Gobin, A. M.; Lee, M. H.; Halas, N. J.; James, W. D.; Drezek, R. A.; West, J. L. *Nano Lett.* **2007**, *7*, 1929. (b) Huang, X.; Jain, P. K.; El-Sayed, I. H.; El-Sayed, M. A. *Lasers Med. Sci.* **2008**, *23*, 217. (c) Lal, S.; Clare, S. E.; Halas, N. J. *Acc. Chem. Res.* **2008**, *41*, 1842.

JA907640H